

Is there Link between the Type of the Volumetric Strain Curve and Elastic Constants, Porosity, Stress and Strain Characteristics ?

V. Palchik

Received: 29 February 2012 / Accepted: 1 May 2012 / Published online: 13 May 2012
© Springer-Verlag 2012

Abstract The stress [crack damage stress (σ_{cd}) and uniaxial compressive strength (σ_c)] and strain characteristics [maximum total volumetric strain (ε_{cd}), axial failure strain (ε_{af}), porosity (n) and elastic constants [elastic modulus (E) and Poisson's ratio (ν)] and their ratios were coordinated with the existence of two different types (type 1 and type 2) of volumetric strain curve. Type 1 volumetric strain curve has a reversal point and, therefore, σ_{cd} is less than the uniaxial compressive strength (σ_c). Type 2 has no reversal point, and the bulk volume of rock decreases until its failure occurs (i.e., $\sigma_{cd} = \sigma_c$). It is confirmed that the ratio between the elastic modulus (E) and the parameter $\lambda = n/\varepsilon_{cd}$ strongly affects the crack damage stress (σ_{cd}) for both type 1 and type 2 volumetric strain curves. It is revealed that heterogeneous carbonate rock samples exhibit different types of the volumetric strain curve even within the same rock formation, and the range of $\sigma_{cd}/\sigma_c = 0.54$ –1 for carbonate rocks is wider than the range ($0.71 < \sigma_{cd}/\sigma_c < 0.84$) obtained by other researchers for granites, sandstones and quartzite. It is established that there is no connection between the type of the volumetric strain curve and values of n , E , σ_{cd} , ν , $E/(1 - 2\nu)$, $M_R = E/\sigma_c$ and E/λ . On the other hand, the type of volumetric strain curve is connected with the values of λ and the ratio between the axial failure strain (ε_{af}) and the maximum total volumetric strain (ε_{cd}). It is argued that in case of small $\varepsilon_{af}/\varepsilon_{cd}$ —small λ , volumetric strain curve follows the type 2.

Keywords Failure strain · Volumetric strain curve · Porosity · Crack damage stress

1 Introduction

Most rock mechanics studies of characteristic stress levels during compression have so far been focused on the crack damage stress (σ_{cd}) and uniaxial compressive strength (σ_c) (e.g., Brace et al. 1966; Bieniawski 1967; Brady and Brown 1993; Martin 1993; Martin and Chandler 1994; Hatzor and Palchik 1997; Pettitt et al. 1998; Eberhardt et al. 1999; Palchik and Hatzor 2002; Cai et al. 2004; Katz and Reches 2004; Palchik 2010a; Stefanov et al. 2011). Martin and Chandler (1994) and Eberhardt et al. (1999) have shown that strength degradation begins with the initiation of the microfracturing process (Nicksiar and Martin 2012) and can end in failure at stresses (σ_{cd}) well below the uniaxial compressive strength (σ_c). They have introduced the term “crack damage stress σ_{cd} ” and have shown that granites become critically damaged at $\sigma_{cd} < \sigma_c$. The crack damage stress σ_{cd} (or stress at the onset of dilation) is the stress level at which the maximum total volumetric strain is attained (Schock et al. 1973; Brace 1978; Paterson 1978; Palchik and Hatzor 2002). Values of $\sigma_{cd} < \sigma_c$ were obtained for sandstones (Brace et al. 1966; Pettitt et al. 1998) and for quartzites (Bieniawski 1967).

On the other hand, Palchik and Hatzor (2002), Palchik (2010a, b) have shown that the crack damage stress (σ_{cd}) can be equal to the uniaxial compressive strength (σ_c) in heterogeneous dolomites, limestones and chalks. When $\sigma_{cd} = \sigma_c$, the maximum total volumetric strain (maximum decrease in rock volume) is attained at uniaxial compressive strength. In this case, the bulk volume of rock decreases until failure occurs.

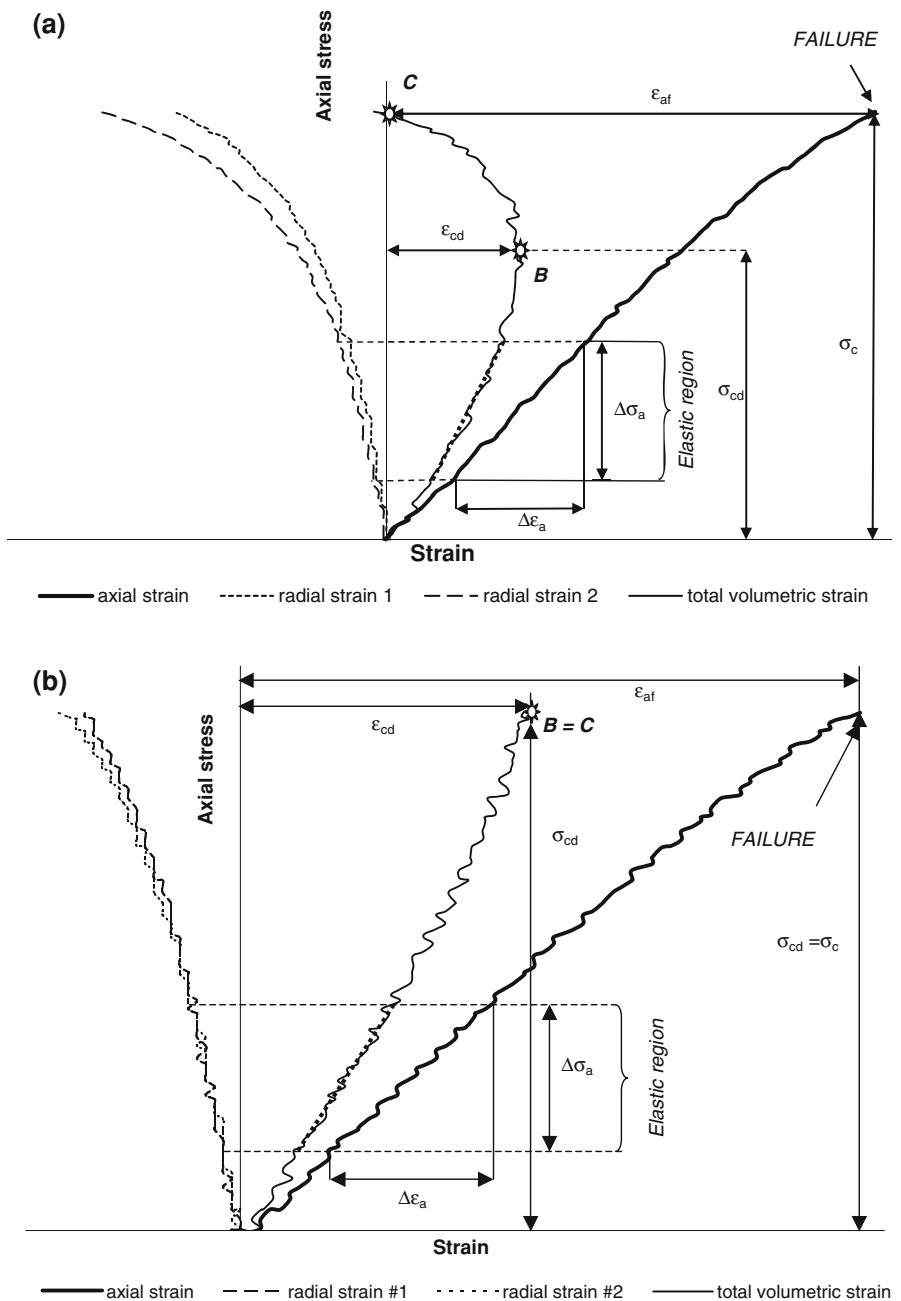
V. Palchik (✉)
Department of Geological and Environmental Sciences,
Ben-Gurion University of the Negev, P.O. Box 653,
84105 Beer-Sheva, Israel
e-mail: vplachek@bgu.ac.il

Thus, there are two different types (Palchik 2010a, b) of volumetric strain curves: type 1 ($\sigma_{cd} < \sigma_c$) and type 2 ($\sigma_{cd} = \sigma_c$). Figure 1 shows these two types—type 1 with a point of reversal (B) in the total volumetric strain curve and $\sigma_{cd} < \sigma_c$; and type 2, where the total volumetric strain has no reversal point and, therefore, $\sigma_{cd} = \sigma_c$ ($B = C$). In Fig. 1, crack damage stress (σ_{cd}) and uniaxial compressive strength (σ_c) are represented by points B and C , respectively. Here, ε_{cd} is the maximum total volumetric strain at crack damage stress (point B), and ε_{af} is the axial failure strain at σ_c (point C).

The heterogeneous carbonate rock samples exhibit different types (type 1 and type 2) of volumetric strain curve

even within the same rock formation. When all studied carbonate rock formations are taken into account, ranges of elastic matrix stiffness [elastic modulus (E)] and porosity (n) are approximately the same for rock samples exhibiting different types of volumetric strain curve: 6,200 MPa $< E < 60,450$ MPa and 6,100 MPa $< E < 64,000$ MPa for type 1 and 2, respectively; 6.1 % $< n < 31.5$ % and 5.4 % $< n < 28.5$ % for type 1 and 2, respectively. Is there a link between the type of the volumetric strain curve and elastic modulus (E) and porosity (n)? Which stress and strain parameters and elastic constants are more connected with the type of stress–volumetric strain response? To the

Fig. 1 Stress–strain diagrams modified after Palchik (2010a). **a** Type 1 of volumetric strain curve ($\sigma_{cd} < \sigma_c$); **b** type 2 of volumetric strain curve ($\sigma_{cd} = \sigma_c$). The total volumetric strain (ε) is calculated as a sum of the component strains: $\varepsilon = \varepsilon_a + \varepsilon_{R1} + \varepsilon_{R2}$, where ε_a is axial strain and ε_{R1} and ε_{R2} are radial strains measured in orthogonal directions (Palchik and Hatzor 2002). The crack damage stress (σ_{cd}) and uniaxial compressive strength (σ_c) are represented by points B and C , respectively. Elastic modulus (E) is calculated as $\Delta\sigma_a/\Delta\varepsilon_a$



author's knowledge, so far no experimental results have been published, which describe the connection between the type of volumetric strain curve and stress and strain parameters, elastic constants and porosity. The goal of this study is to define how the type of the volumetric strain curve is connected with these parameters, elastic constants and their ratios.

2 Testing and Test Results

Sixty carbonate rock samples were used in this study to define the connection of elastic constants and stress and strain parameters with the type of the volumetric strain curve. The preparation of these samples and testing procedure are presented in detail elsewhere (Palchik 2010a, 2011). Table 1 shows types of the volumetric strain curves, value of $\lambda = n/\varepsilon_{cd}$, elastic modulus (E), crack damage stress (σ_{cd}), uniaxial compressive strength (σ_c), porosity (n), Poisson's ratio (ν), ratio between the axial failure strain (ε_{af}) and maximum volumetric strain (ε_{cd}), and ratio between the crack damage stress (σ_{cd}) and uniaxial compressive strength (σ_c) for each of the studied 60 samples.

The values of elastic modulus (E) and Poisson's ratio (ν) were calculated by using linear regressions along linear portions of stress–axial strain curves and radial strain–axial strain curves, respectively. The elastic modulus (E) is the slope of linear portion (elastic region) of the axial stress–strain curve (see Fig. 1): $E = \Delta\sigma_a/\Delta\varepsilon_a$ where $\Delta\sigma_a$ and $\Delta\varepsilon_a$ are changes in axial stress and strain, respectively. Poisson's ratio (ν) is the slope of linear portion of the radial strain–axial strain curve: $\nu = -0.5 (\Delta\varepsilon_{R1} + \Delta\varepsilon_{R2})/\Delta\varepsilon_a$ where $\Delta\varepsilon_{R1}$ and $\Delta\varepsilon_{R2}$ are changes in radial strains measured in orthogonal directions.

Porosity was calculated as $n = [1 - (\rho/G_s)] \times 100\%$ where ρ is dry bulk density and $G_s = 2.7\text{--}2.8\text{ g/cm}^3$ is specific gravity of the solids. Dry bulk density (ρ) of rock sample is defined as M/V_b where M and V_b are dry mass and bulk volume of sample, respectively. The porosity was also measured in our laboratory by Helium porosimeter (Core Test Inc., model PHI-220). The relative errors between calculated porosity and porosity measured by Helium porosimeter are less than 15–18%. Note that some of the studied carbonate rocks (for example, Adulam chalk) exhibit very good linear correlation ($R^2 = 0.99$) between calculated and measured porosity (Palchik and Hatzor 2004).

The value of n in Table 1 ranges from 5.4 to 31.5%. The ranges of $\varepsilon_{af}/\varepsilon_{cd}$ and σ_{cd}/σ_c ratios are 1.51–6.91 and 0.54–1, respectively. The latter ($\sigma_{cd}/\sigma_c = 0.54\text{--}1$) differs from the values of $\sigma_{cd}/\sigma_c = 0.71\text{--}0.84$ obtained by Brace et al. (1966), Bieniawski (1967), Martin (1993), Pettitt et al. (1998), Eberhardt et al. (1999), Heo et al. (2001),

Katz and Reches (2004) for granites, sandstones and quartzite (see Fig. 2a). Figure 2a presents histogram showing the distribution of σ_{cd}/σ_c for studied rock samples at class intervals of 0.05. In Fig. 2a, 50 of 60 samples exhibit σ_{cd}/σ_c values located outside the range of σ_{cd}/σ_c obtained for granites, sandstones and quartzite. The number of rocks samples within the interval $0.95 < \sigma_{cd}/\sigma_c \leq 1$ is 27 (45%) of 60 samples. The number of rocks samples in other class intervals of σ_{cd}/σ_c is less than in the interval 0.95–1.

The ranges of the elastic modulus (E), Poisson's ratio (ν), crack damage stress (σ_{cd}) and uniaxial compressive strength (σ_c) for the studied 60 samples are presented in Fig. 2b. Of course, weak-to-strong and very strong studied rock samples exhibit different grain/cement configurations, various grain contact types, different grain sizes and porosity, etc. that results in difference in rock deformability. For this reason, maximum volumetric strain (ε_{cd}), axial failure strain (ε_{af}) and parameter λ have wide ranges: $0.036\% < \varepsilon_{cd} < 0.9\%$, $0.11\% < \varepsilon_{af} < 1.97\%$ and $23 < \lambda < 585.3$. In this paper, it is established that the combinations of parameter λ and ratio between ε_{af} and ε_{cd} for carbonate rocks are pronouncedly connected with the type of volumetric strain curve (see Sect. 5).

It is clear from Table 1 that rock samples exhibit different types of volumetric strain curve even within the same carbonate rock formation. 24 (40%) of 60 studied rock samples exhibit total volumetric strain curve of type 2. The number of rock samples exhibiting different types (1 and 2) of the volumetric strain curve within each of the studied rock formations is presented in Fig. 2b. For example, 7 (58%) of 12 Adulam chalk samples, 2 (40%) of 5 Aminadav dolomite samples, 6 (32%) of 19 Bina limestone samples, 5 (83%) from 6 Nekorot limestone samples, 3 (43%) from 7 Yagur dolomite samples and 1 (25%) from 4 Yarka limestone samples exhibit type 2 of volumetric strain behavior. Figure 2b also shows that the rock samples with NX size (diameter of 54 mm and length/diameter ratio of 2) were prepared following ISRM suggested methods.

3 Parameters n , λ , Ω , ε_{af} and ε_{cd}

Porosity n is a measure of void space (pores and open cracks) and represents a ratio between the void space (V_p) and bulk volume (V_b).

$$n = \frac{V_p}{V_b} \quad (1)$$

Since V_b is the initial volume of a sample before loading and, therefore, does not reflect the change in volume due to compression, Palchik and Hatzor (2002) and Palchik (2010a) have proposed to use the maximum decrease

Table 1 Types of volumetric strain curves and values of λ , E , σ_{cd} , σ_c , n , ν , $\varepsilon_{af}/\varepsilon_{cd}$ and σ_{cd}/σ_c

Rock	Sample	Type	λ	E (MPa)	σ_{cd} (MPa)	σ_c (MPa)	n (%)	ν	$\varepsilon_{af}/\varepsilon_{cd}$	σ_{cd}/σ_c
AD	Rc1	2	134.3	17,400	53.2	53.2	21.5	0.23	2.00	1
	Rc2	1	273.8	9,300	18.3	21	31.5	0.2	3.22	0.87
	Rc3	2	101.9	16,000	51	51	23.3	0.26	1.79	1
	Rc4	2	171.8	11,700	31.9	31.9	28.5	0.2	1.93	1
	Rc6	1	188.6	19,250	44.9	63.3	20.7	0.26	3.73	0.71
	Rc7	1	157.9	9,500	29.8	32.1	30	0.21	2.16	0.93
	Rc8	2	100.2	17,300	60.3	60.3	21.9	0.2	1.7	1
	Rc9	2	146.5	20,500	63.1	63.1	19.6	0.27	2.31	1
	St1a	1	186.9	15,300	48.3	50.9	20.4	0.27	3.39	0.95
	St1b	1	144.9	15,400	45.6	53.7	20	0.23	2.83	0.85
	St2a	2	111.5	14,300	52.3	52.3	20.7	0.2	2.15	1
St2b	2	149.1	10,700	37.4	37.4	23.7	0.22	2.14	1	
AM	Ad5	1	107.1	56,000	85	97.8	6.4	0.37	3.33	0.87
	Ad15	1	242.1	29,000	57	67.2	21.8	0.26	2.78	0.85
	Ad43	2	25.5	64,000	273.9	273.9	5.4	0.27	2.26	1
	Ad80	2	48	58,500	174.2	174.2	6.4	0.28	2.36	1
	Ad83	1	219.4	18,000	43	61.6	15.4	0.25	4.86	0.7
BEM	Bm2	1	473.6	38,100	40	71.5	17.1	0.4	6.91	0.56
	Bm3	1	329.1	21,400	43.7	46	29.3	0.22	2.47	0.95
BIN	Bina1	1	42.8	60,450	170	187.2	6.1	0.23	2.3	0.91
	Bina2	2	115.5	34,400	77	77	15.7	0.25	2.33	1
	Bina5	2	139.3	38,700	80	80	13.9	0.24	2.1	1
	Bina6	1	89.3	24,800	65	89	10.7	0.27	4	0.73
	Bina7	2	108.2	25,000	64	64	14.3	0.2	2.2	1
	Th5-15	1	142.9	37,700	78	84	13.6	0.27	2.63	0.93
	Th3-24	1	315.7	10,000	12.3	15.4	21.8	0.26	2.61	0.8
	Th5-13	1	522.6	24,000	22.9	31.3	21.4	0.31	3.41	0.73
	Tb2-5a	1	90.3	25,900	85	90.5	15.4	0.22	2.42	0.94
	Tb2-12	1	75.1	25,300	89.3	104.2	13.2	0.24	3.22	0.86
	Tb3-2	2	51	41,830	139	139	7.5	0.26	2.46	1
	Tb3-4	1	92.8	32,130	86.7	100.4	11.8	0.25	3.21	0.86
	Tb3-9	1	196.4	25,550	38.8	44.5	15.7	0.22	2.35	0.87
	Tb8-16	1	125.9	26,590	71.8	77.9	17.5	0.23	2.48	0.92
	B1	1	197.4	43,100	51	66.5	7.5	0.4	5	0.77
	B2	1	585.3	20,900	13.6	25	21.1	0.25	4.44	0.54
	B3	2	314.6	21,000	35	35	26.4	0.31	2.26	1
B5	2	122.5	35,200	98	98	16.8	0.25	2.12	1	
B7	1	54.5	10,900	53	54.4	20	0.15	2.13	0.97	
NK	Gn2-1b	2	48.4	47,000	177	177	11.4	0.23	1.83	1
	Gn2-4a	2	80.1	44,600	141	141	13.2	0.25	2	1
	Gn2-5b	2	56.2	48,600	162	162	11.1	0.25	1.85	1
	Gn3-2a	2	77.6	44,800	150	150	12.5	0.24	2.24	1
	Gn3-2c	2	73	44,400	163	163	13.6	0.25	2.13	1
	Gn3-3a	1	68.9	49,000	175	178	11.8	0.28	2.3	0.98
SOR	Bz5-16	1	108	24,300	64	78	17.5	0.22	2.47	0.82
	Bz2-61	1	102	22,300	50	85.8	13.6	0.2	3.76	0.58
	Bz2-35a	1	187.1	16,200	22	32	15.7	0.26	3.1	0.69
YAG	Yn1	1	150.7	33,290	76.5	112	16.4	0.24	3.55	0.68

Table 1 continued

Rock	Sample	Type	λ	E (MPa)	σ_{cd} (MPa)	σ_c (MPa)	n (%)	ν	$\varepsilon_{af}/\varepsilon_{cd}$	σ_{cd}/σ_c
	Yn3	1	23	7,200	97.8	105	18.9	0.13	2.1	0.93
	Yn4	2	27.8	6,100	75	75	25	0.13	1.51	1
	Yn5	1	25.5	7,000	99.6	115	19.6	0.17	2.56	0.87
	Yn6	1	197.8	47,700	68.7	77	12.9	0.25	2.71	0.89
	Ca3541	2	55.1	54,000	173.9	173.9	8.2	0.19	2.32	1
	Ca5671	2	119.9	35,500	60	60	16.8	0.19	1.66	1
YAN	Yan2	1	392	35,400	32.8	37	16.1	0.32	2.68	0.89
	Yan3	1	382.1	27,700	21.7	25	16.4	0.2	3.05	0.87
YAR	Yarka1	1	46.4	6,500	37.7	38.7	15.7	0.15	1.86	0.97
	Yarka 2	1	83.4	6,200	29	38.7	17.9	0.24	3.46	0.75
	Yarka3	2	57.2	6,200	41	41	17.9	0.18	2.21	1
	Yarka4	1	47.8	8,400	59.4	71	16.4	0.19	3.11	0.84

AD Adulam chalk, AM Aminadav dolomite, BEM Beit-Meir dolomite, BIN Bina limestone, NK Nekorot limestone, SOR Sorek limestone, YAG Yagur dolomite, YAN Yanuach limestone, YAR Yarka dolomite

λ ratio between porosity (n) and maximum volumetric strain (ε_{cd}), E elastic modulus, σ_{cd} crack damage stress, σ_c uniaxial compressive strength, n porosity, ν Poisson’s ratio, $\varepsilon_{af}/\varepsilon_{cd}$ ratio between axial failure strain (ε_{af}) and maximum volumetric strain (ε_{cd}), σ_{cd}/σ_c ratio between crack damage stress (σ_{cd}) and uniaxial compressive strength (σ_c)

(ΔV_c) in bulk volume instead of V_b . In this case, Eq. (1) can be rewritten as (Palchik 2010a):

$$\lambda = \frac{V_p}{\Delta V_c} = \frac{n}{\varepsilon_{cd}} \tag{2}$$

where ΔV_c is the maximum decrease in a sample volume, which is attained at the maximum total volumetric strain ε_{cd} (at the crack damage stress σ_{cd}).

The inverse value of λ is a specific maximum decrease (Ω) in a sample volume (maximum decrease in volume per unit pore volume):

$$\Omega = \frac{1}{\lambda} = \frac{\Delta V_c}{V_p} \tag{3}$$

Palchik (2010a) has found a power dependence between E/λ and crack damage stress (σ_{cd}) for type 2. This relation is confirmed in this paper not only for type 2, but also for type 1 (see Fig. 3a), and it is established that the value of σ_{cd} is correlated with E/λ rather than E/n when two types of volumetric curve are considered. Indeed, the dependence $\sigma_{cd}-(E/\lambda)$ in Fig. 3a exhibits $R^2 = 0.91$, whereas the best R^2 (Fig. 3b) for the relation $\sigma_{cd}-(E/n)$ is only 0.61. The dependence between σ_{cd} and E/λ presented in Fig. 3a for two types (type 1 and type 2) can be described as:

$$\sigma_{cd} = k_1 \left(\frac{E}{\lambda} \right)^{k_2} \tag{4}$$

where k_1 and k_2 are empirical coefficients: $k_1 = 1.93$ and $k_2 = 0.654$ for all studied carbonate rocks exhibiting types 1 and 2.

The relationships between porosity (n) and elastic modulus (E) and uniaxial compressive strength (σ_c) for all

studied samples are presented in Fig. 4. The latter demonstrates that the values of E and σ_c tend to decrease with increasing porosity (n). However, elastic modulus and σ_c only partly depend on the porosity ($R^2 = 0.57-0.68$ is relatively small), and there are no simple explicit dependences (with reasonable regression coefficients) between n and E and σ_c .

Palchik (2007, 2011) proposed mathematical relation between $M_R = E/\sigma_c$ and failure axial strain (ε_{af}) for carbonate rock exhibiting $\varepsilon_{af} \leq 1\%$. According to this relation, M_R increases exponentially with decreasing ε_{af} :

$$M_R = \frac{2k}{\varepsilon_{af}(1 + e^{-\varepsilon_{af}})} \tag{5}$$

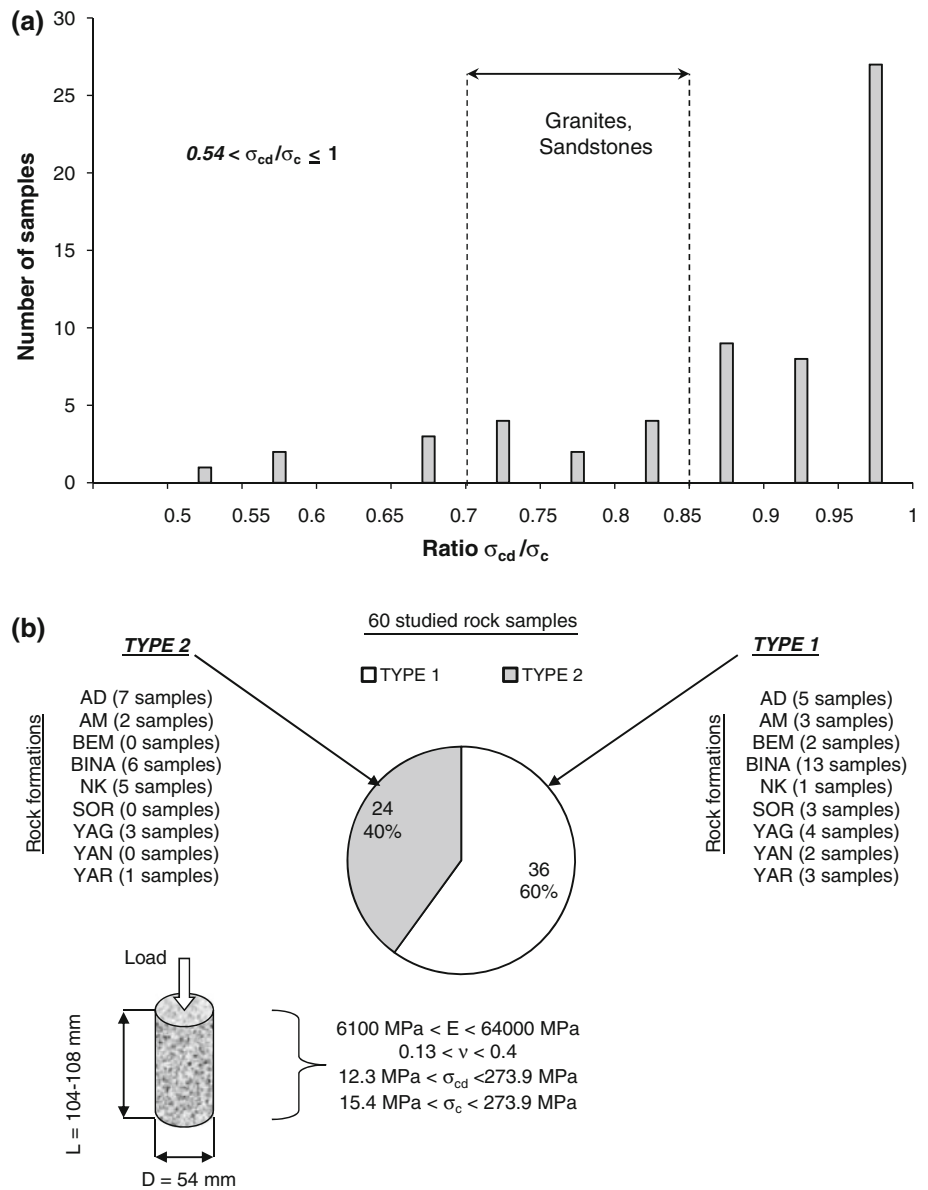
where $k = 100$ is the conversion coefficient, since ε_{af} is measured in %. When the value of M_R is known, ε_{af} (%) is obtained from Eq. (5) as

$$\varepsilon_{af} = \frac{k}{M_R - 0.46k} \tag{6}$$

since the expansion of the expression $2/(1 + e^{-\varepsilon_{af}})$ using Taylor’s theorem shows that the value of $2/(1 + e^{-\varepsilon_{af}}) = 1 + 0.46\varepsilon_{af}$.

In this paper, it is established that M_R is correlated not only with maximum deformation in the axial direction (ε_{af}) but also and maximum volumetric deformation (ε_{cd}). This fact is confirmed in Fig. 5. The latter shows that good correlation ($R^2 = 0.85$) between maximum volumetric strain (ε_{cd}) and value of M_R exists. The relation between ε_{cd} and M_R follows power law and has following mathematical form:

Fig. 2 Description of studied rock samples. **a** Histogram showing class intervals of ratio σ_{cd}/σ_c ; **b** number of rock samples exhibiting different types (1 and 2) of volumetric strain curve within each of studied rock formations, dimensions of rock samples and ranges of E , ν , σ_{cd} and σ_c



$$\epsilon_{cd} = aM_R^{-b} \tag{7}$$

where a and b are empirical coefficients: $a = 96.7$ and $b = 1.13$.

4 Definition of Parameters Correlated with the Type of Volumetric Strain Curve

4.1 Porosity and λ

From Fig. 6a it is clear that 52 (86.6 %) of 60 samples have porosity in the interval 10–30 %. Only seven samples (11.7 %) exhibit relatively small porosity of $n = 5$ –10 %, and only one sample (1.7 %) exhibits large $n > 30$ %. The

histogram of n distribution in Fig. 6a also shows that the type of volumetric strain curve is not linked with the values of the initial porosity (n). Indeed, the difference between the number of samples exhibiting type 1 (10 samples) and type 2 (11 samples) behavior is insignificant when the values of $5\% < n < 15\%$. When $15\% < n < 35\%$, the number of samples exhibiting type 1 (26 samples) and type 2 (13 samples) behavior simultaneously increases. Figure 8b shows that there is no correlation between the porosity (n) and the ratio σ_{cd}/σ_c (best $R^2 = 0.0021$ is very small).

On the other hand, the type of volumetric strain curve is linked with the values of the parameter λ (Fig. 6b). From Fig. 6b it is clear that for small λ values ($0 < \lambda < 150$), the number of samples of type 1 (18 samples) is less than that

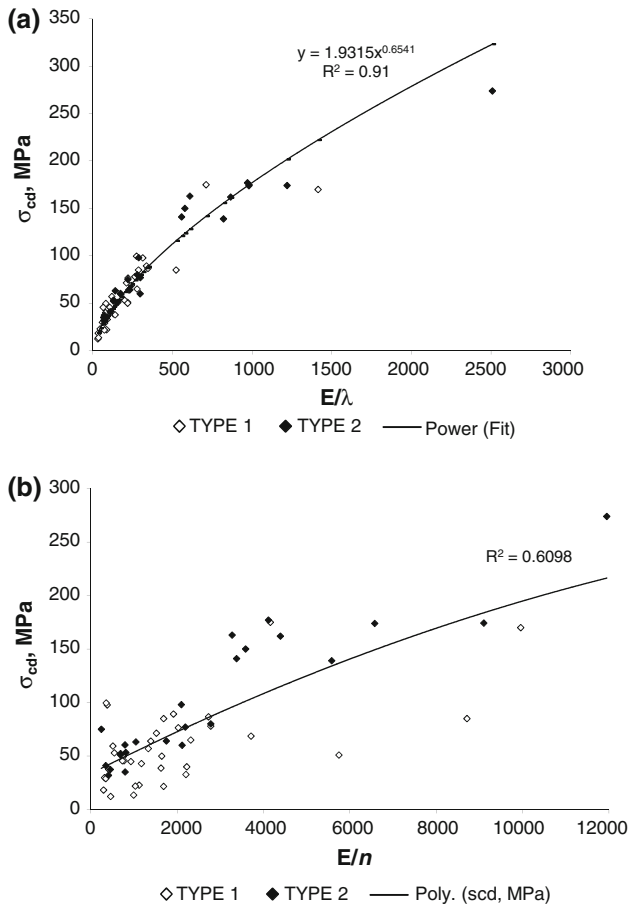


Fig. 3 Relations between σ_{cd} and values of E/λ and E/n for two types of volumetric strain curve. **a** E/λ ($R^2 = 0.91$); **b** E/n ($R^2 = 0.61$)

of samples of type 2 (22 samples). Note that 23 samples (98 %) of 24 exhibiting type 2 behavior have small λ in the range $0 < \lambda < 200$. For large $150 < \lambda < 600$, the number

Fig. 4 Relations between porosity (n) and elastic modulus (E) and uniaxial compressive strength (σ_c) for all studied rocks

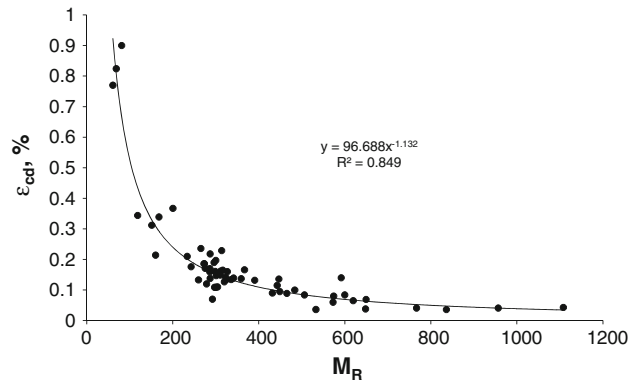
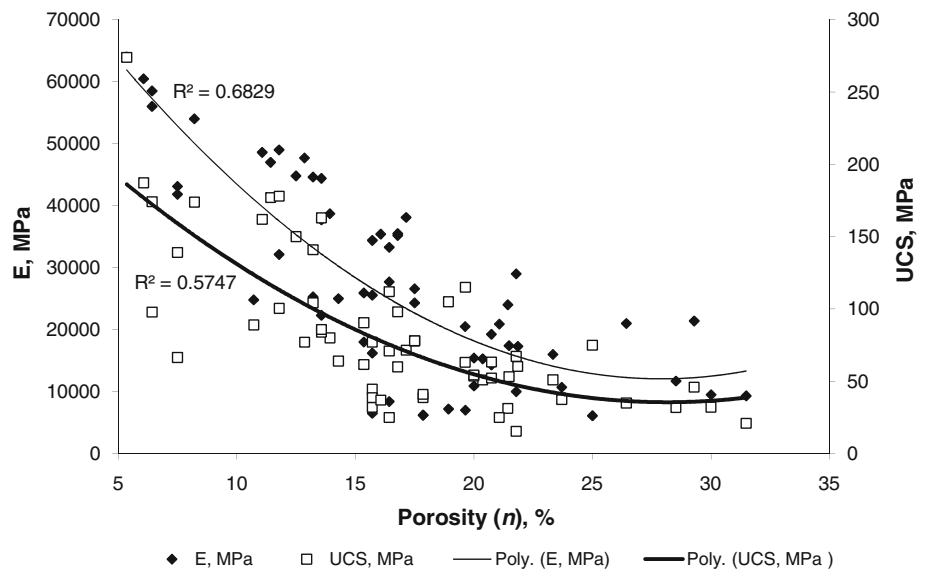


Fig. 5 Relation between $M_R = E/\sigma_c$ and maximum volumetric total strain (ϵ_{cd}) for all studied rocks

of samples (18) exhibiting type 1 remains unchanged, whereas the number of samples exhibiting type 2 behavior is rapidly reduced from 22 to 2. Thus, the probability of type 2 behavior of the total volumetric strain curve increases with decreasing λ value. Figure 7 shows that there is a correlation between σ_{cd}/σ_c and λ . In Fig. 7, λ tends to a decrease from 585.3 to 22.9 with σ_{cd}/σ_c value increasing from 0.544 to 1. The small $R^2 = 0.31$ can be explained by a combined influence of λ and $\epsilon_{af}/\epsilon_{cd}$ on the value of σ_{cd}/σ_c . The correlations between the type of volumetric strain curve and $\epsilon_{af}/\epsilon_{cd}$, and $\lambda - \epsilon_{af}/\epsilon_{cd}$ combinations are presented below in Sects. 4.3 and 5, respectively.

4.2 E , σ_{cd} , ν , $E/(1 - 2\nu)$, $M_R = E/\sigma_c$ and E/λ

The values of such important mechanical parameters as E , σ_{cd} , ν , $M_R = E/\sigma_c$ and E/λ were analyzed, and histograms of the distribution of each of these parameters for two different types of volumetric strain curve were plotted.

Fig. 6 Histogram of distributions of n and λ for two different types (type 1 and type 2) of total volumetric strain curves: **a** n , **b** λ

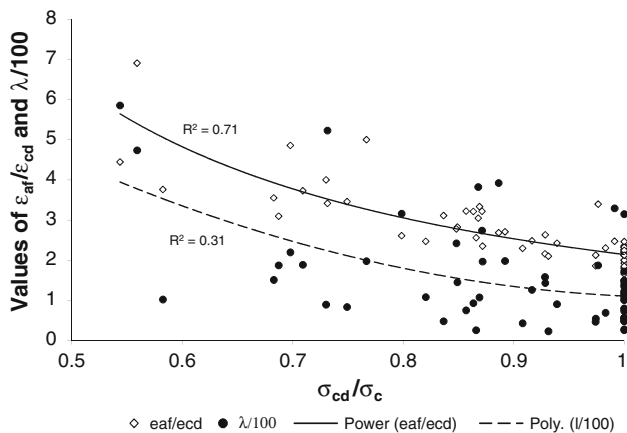
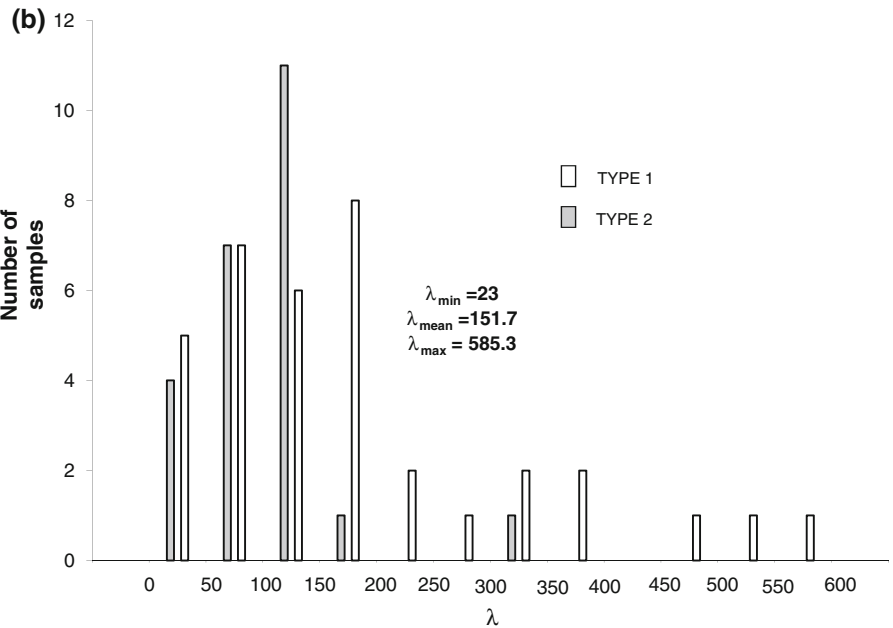
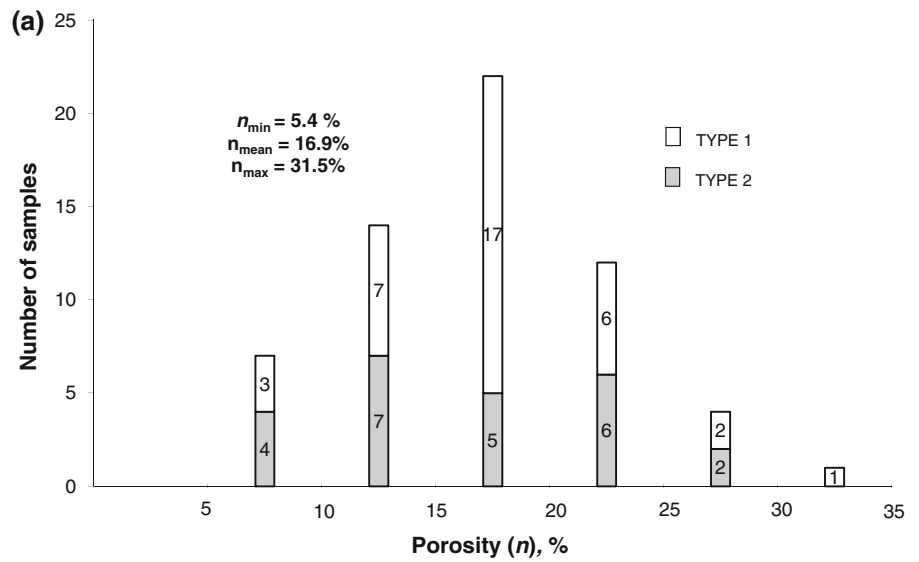
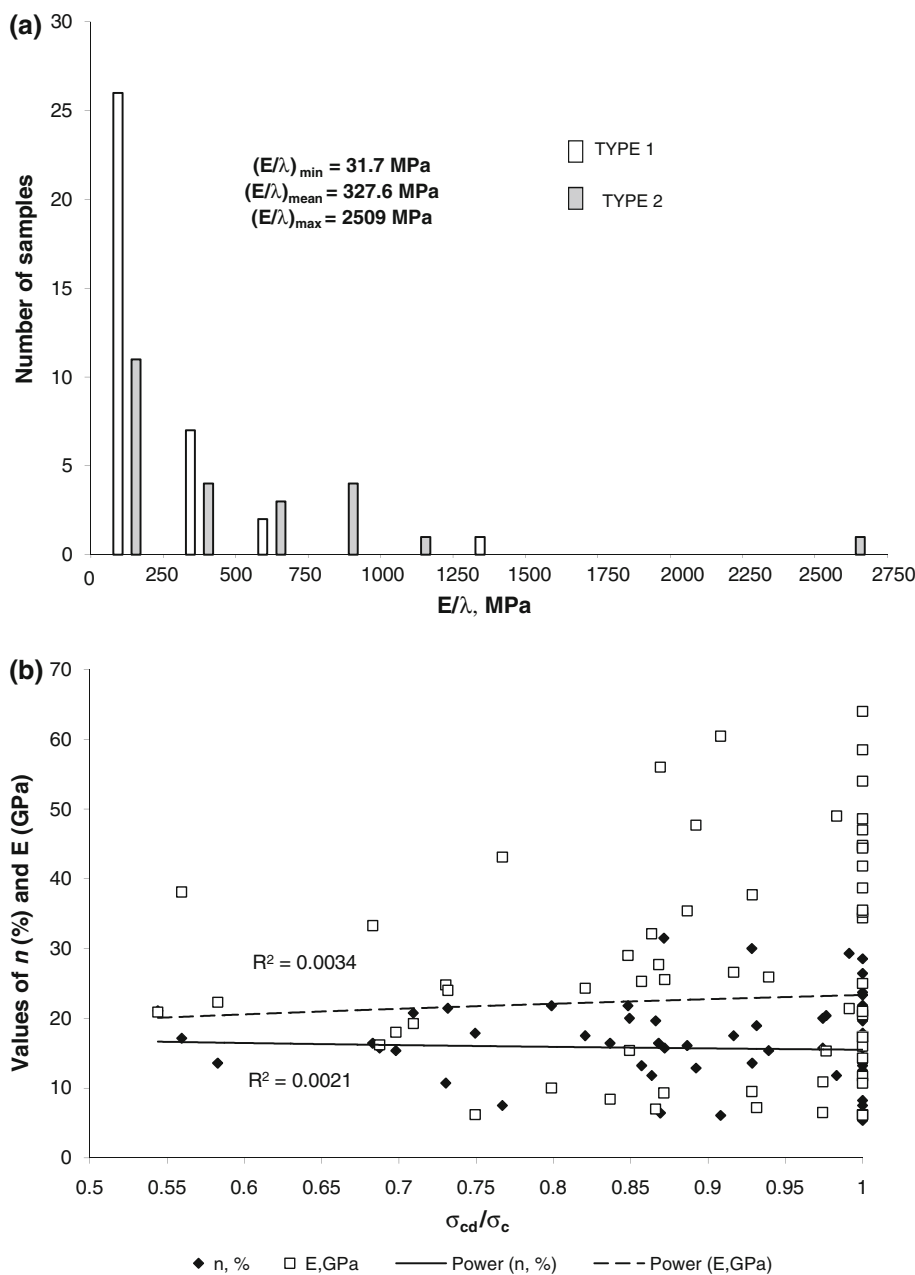


Fig. 7 Relations between σ_{cd}/σ_c and $\epsilon_{af}/\epsilon_{cd}$ ($R^2 = 0.71$) and λ ($R^2 = 0.31$)

Elastic modulus (E) is a measure of overall rock stiffness, including the stiffness of grain to grain contacts and intergranular matrix. The elastic modulus (E) and Poisson's ratio (ν) are extensively used in rock engineering when deformations of different structural elements of underground storages, caverns, tunnels or mining openings must be computed. The crack damage stress (σ_{cd}) and E/λ that strongly affects σ_{cd} are important for accurate assessment of the volumetric strain response of the rock to excavation-induced stress concentration. The ratio $M_R = E/\sigma_c$ is also important parameter since latter is well-correlated with axial failure strain and maximum volumetric strain (see Sect. 3). The axial failure strain and maximum volumetric strain are needed for the prediction of squeezing potential in tunnels and volumetric strain response of the

Fig. 8 Correlation between the type of volumetric strain curve and some parameters. **a** Histogram of E/λ distribution for two different types of total volumetric strain curves; **b** there are no correlations between E , n and σ_{cd}/σ_c ($R^2 = 0.0021-0.0034$)



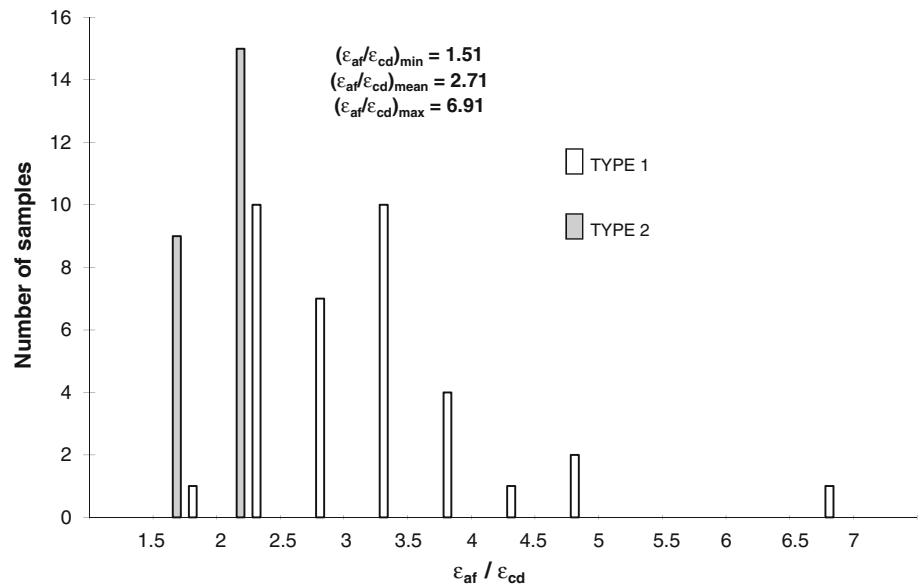
overburden, respectively. The value of elastic expression of $E/(1 - 2\nu)$ was also analyzed since this expression is often used in the theory of elasticity. In particular, Palchik and Hatzor (2002) have experimentally found that $E/(1 - 2\nu)$ is correlated with the ratio $\sigma_{cd}/\epsilon_{cd}$.

However, as a result of statistical analysis, it is established that the type of volumetric strain curve does not correlate with the above-mentioned parameters and expression of $E/(1 - 2\nu)$. By way of example, see Fig. 8a where the distribution of E/λ is presented. Here, 59 of 60 rock samples exhibit $0 < E/\lambda < 1,500$. For small $0 < E/\lambda < 750$, 35 and 18 samples exhibit type 1 and type 2 behavior,

respectively. This fact suggests that smaller values of E/λ correspond to type 1 and, probably, larger values of E/λ may correspond to type 2. However, for large $750 < E/\lambda < 1,500$, the increase in the number of samples exhibiting type 2 behavior does not occur (on the contrary, this number decreases from 18 to 5). Thus, a correlation between the type of volumetric strain curve and E/λ does not exist.

Note also that the values of E , σ_{cd} , ν , $E/(1 - 2\nu)$, $M_R = E/\sigma_c$ and E/λ are not correlated with the ratio σ_{cd}/σ_c . For example, Fig. 8b demonstrates that the best $R^2 = 0.0034$ obtained while examining the dependence between σ_{cd}/σ_c and elastic modulus (E) is very small.

Fig. 9 Histogram of $\varepsilon_{af}/\varepsilon_{cd}$ distribution for two different types (type 1 and type 2) of total volumetric strain curves



4.3 $\varepsilon_{af}/\varepsilon_{cd}$

Palchik (2010a) has shown that the axial failure strain (ε_{af}) is 1.51–2.46 times the maximum volumetric strain (ε_{cd}) when $\sigma_{cd} = \sigma_c$ (type 2). In this study it was determined that the value of $\varepsilon_{af}/\varepsilon_{cd}$ for rock samples of type 1 is larger ($1.86 < \varepsilon_{af}/\varepsilon_{cd} < 6.91$) and that there is a pronounced link between $\varepsilon_{af}/\varepsilon_{cd}$ and the type of volumetric strain curve. The histogram of $\varepsilon_{af}/\varepsilon_{cd}$ distribution for two types of volumetric strain curve is presented in Fig. 9. When small $1.5 < \varepsilon_{af}/\varepsilon_{cd} < 2.5$, 11 and 24 samples exhibit type 1 and 2, respectively. For large $2.5 < \varepsilon_{af}/\varepsilon_{cd} < 7$, the number of samples of type 1 rapidly increases up to 25 and there are no samples of type 2 at all. Thus, small values of $\varepsilon_{af}/\varepsilon_{cd}$ correspond to type 2, while large values of $\varepsilon_{af}/\varepsilon_{cd}$ correspond to type 1. This fact is confirmed by Fig. 7 where $\varepsilon_{af}/\varepsilon_{cd}$ decreases with increasing σ_{cd}/σ_c and reaches its minimum values at $\sigma_{cd}/\sigma_c = 1$ (for type 2). In Fig. 7, correlation ($R^2 = 0.71$) between the values of $\varepsilon_{af}/\varepsilon_{cd}$ and σ_{cd}/σ_c is obtained.

5 Discussion

It is established that the parameter λ is an important parameter: the ratio E/λ strongly influences the crack damage stress (σ_{cd}), and the type of volumetric strain curve correlates with λ value.

Note, however, that the type of volumetric strain curve is partly connected not only with the parameter λ , but also with the ratio $\varepsilon_{af}/\varepsilon_{cd}$. Therefore, a statistical analysis of $\varepsilon_{af}/\varepsilon_{cd}$ – n/ε_{cd} combinations was performed, and it was found

that the volumetric strain curve follows the type 2 curve when the following inequality is satisfied:

$$\frac{n}{\varepsilon_{cd}} \leq \alpha \left[1 - \ln \left(\frac{\varepsilon_{af}}{\varepsilon_{cd}} \right) \right] \quad (8)$$

Otherwise, volumetric strain curve follows the type 1. In Eq. (8), $\alpha = 769.2$ is a derived dimensionless statistical coefficient.

The inequality (Eq. 8) is obtained by successive comparisons $\varepsilon_{af}/\varepsilon_{cd}$ and $\lambda = n/\varepsilon_{cd}$ values and correlation of their differences with facts of the existence of type 1 or type 2 of the volumetric strain curve. To determine the mathematical form of the right-hand part of the inequality, different mathematical laws (linear, power, exponential, polynomial and logarithmic) and their combinations were examined.

The obtained inequality is valid for 53 (88 %) of the 60 studied samples. Values of $F = \alpha [1 - \ln(\varepsilon_{af}/\varepsilon_{cd})]$ and λ for these 53 rock samples are shown graphically in Fig. 10a. Here, the value of F varies between –717 and 451.6 with the mean of 22.1, whereas the value of λ ranges from 25.5 to 585.3. The difference between F and λ for the same 53 rock samples is presented in Fig. 10b. The latter demonstrates that samples having $F - \lambda \geq 0$ exhibit type 2 behavior, whereas the volumetric strain curves of samples exhibiting $F - \lambda < 0$ follow type 1 curve.

The equivocal results of calculation according to Eq. (8) for other seven (Bina 1, B3, B7, Gn3-3a, yn3 and yn5 and Yarka1) of 60 samples can be explained. Three samples (B7, gn3-3a and Yarka 1) exhibit type 1 behavior with very small relative errors ($1.7 < \Delta < 2.6$ %) between σ_{cd} and σ_c , and, therefore, Eq. (8) predicts these samples as samples of type 2 (i.e., $\sigma_{cd} = \sigma_c$). Two (yn3 and yn5) samples

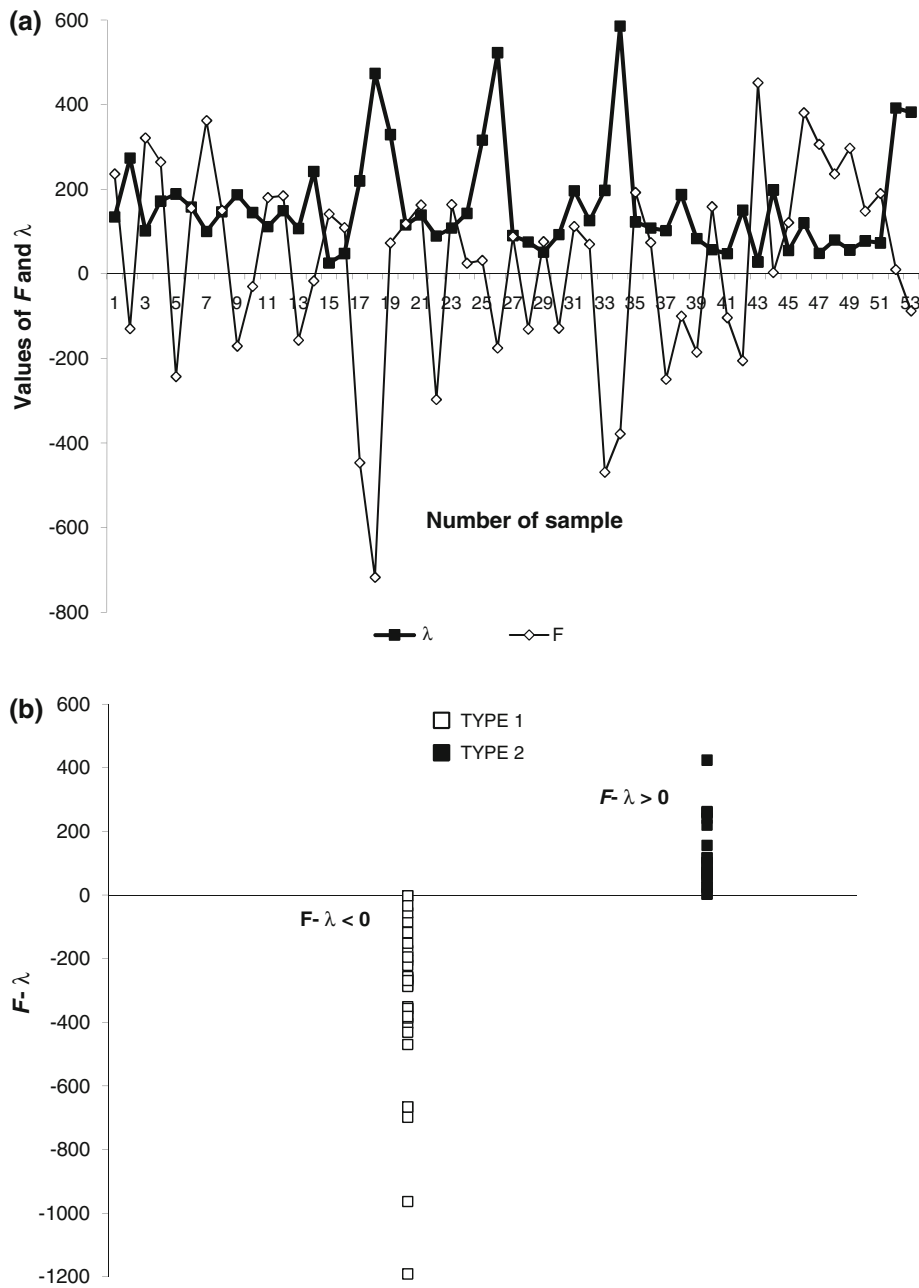


Fig. 10 Variations in values of $F = \alpha [1 - \ln(\epsilon_{af}/\epsilon_{cd})]$, $\lambda = n/\epsilon_{cd}$, and $F - \lambda$ for 53 rock samples. **a** Values of F and λ for each sample; **b** values of difference between F and λ for two different types of volumetric strain curve

have maximum values of failure strain ($\epsilon_{af} = 1.73$ and 1.97% , respectively), which are outliers. The last two samples of Bina limestone (Bina 1 and b3) have initial veins which probably distorted the volumetric strain distribution.

From Eq. (8) it is clear that a decrease in the ratio n/ϵ_{cd} contributes to the formation of type 2. Eq. (8) also shows that the decrease in the ratio $\epsilon_{af}/\epsilon_{cd}$ leads to an increase in the value of the right-hand part of the inequality and, hence, contributes to the formation of type 2. This fact suggests that in case of small $\epsilon_{af}/\epsilon_{cd}$ —small n/ϵ_{cd} , the

probability of the formation of type 2 of the volumetric strain curve is increased. The ratio $\epsilon_{af}/\epsilon_{cd}$ is a manifestation of maximum deformability in the axial direction related to the maximum volumetric change of rock sample.

6 Conclusions

The correlation of stress and strain parameters, porosity, elastic constants and their ratios with the facts of the

existence of type 1 or type 2 volumetric strain curve was performed. The main conclusions are the following:

- The heterogeneous carbonate rock samples have different types of the volumetric strain curve even within the same rock formation. 36 (60 %) and 24 (40 %) of 60 studied rock samples belong to type 1 and type 2, respectively. The studied carbonate rocks exhibit a wide range of $\sigma_{cd}/\sigma_c = 0.54\text{--}1$, whereas this range for granites, sandstones and quartzite is only 0.71–0.84.
- It is established that the ratio between the elastic modulus (E) and the parameter $\lambda = n/\varepsilon_{cd}$ strongly influences the crack damage stress (σ_{cd}) not only for rocks of type 2 (when $\sigma_{cd} = \sigma_c$), but also for rocks of type 1 (when $\sigma_{cd} < \sigma_c$). The crack damage stress (σ_{cd}) increases according to a power law with increasing E/λ for rocks exhibiting two different types of the volumetric strain curve.
- It is found that there is no link between the type of volumetric strain curve and the values of porosity (n), elastic modulus (E), crack damage stress (σ_{cd}), Poisson's ratio (ν), $E/(1 - 2\nu)$, $M_R = E/\sigma_c$ and E/λ .
- A pronounced link between the type of volumetric strain curve and combinations of ratios n/ε_{cd} and $\varepsilon_{af}/\varepsilon_{cd}$ is established. It is defined that in case of small $\varepsilon_{af}/\varepsilon_{cd}$ —small n/ε_{cd} the probability of type 2 behavior of the volumetric strain curve is higher.

References

- Bieniawski ZT (1967) Mechanism of brittle fracture of rock. *Int J Rock Mech Min Sci* 4(4):395–430
- Brace WF (1978) Volume changes during fracture and frictional sliding: a review. *PAGEOGH*. 116:603–614
- Brace WF, Paulding B, Scholz C (1966) Dilatancy in the fracture of crystalline rocks. *J Geophys Res* 71(16):3939–3953
- Brady BHG, Brown ET (1993) *Rock mechanics for underground mining*, 2nd edn. Chapman and Hall, London, p 571
- Cai M, Kaiser PK, Tasaka Y, Maejima T, Morioka H, Minami M (2004) Generalized crack initiation and crack damage stress thresholds of brittle rock masses near underground excavations. *Int J Rock Mech Min Sci* 41(5):833–847
- Eberhardt E, Stead D, Stimpson B (1999) Quantifying progressive pre-peak brittle fracture damage in rock during uniaxial compression. *Int J Rock Mech Min Sci* 36:361–380
- Hatzor YH, Palchik V (1997) The influence of grain size and porosity on crack initiation stress and critical flaw length in dolomites. *Int J Rock Mech Min Sci* 34(5):805–816
- Heo JS, Cho HK, Lee CI (2001) Measurement of acoustic emission and source location considering anisotropy of rock under triaxial compression. In: Sarkka P, Eloranta P (eds) *Rock mechanics a challenge for society*. Swets and Zeitlinger Lisse, Espoo, pp 91–96
- Katz O, Reches Z (2004) Microfracturing, damage and failure of brittle granites. *J Geophys Res* 109(B1)
- Martin CD (1993) Strength of massive Lac du Bonnet granite around underground openings. PhD thesis, Department of Civil and Geological Engineering, University of Manitoba, Winnipeg
- Martin CD, Chandler NA (1994) The progressive fracture of Lac du Bonnet Granite. *Int J Rock Mech Min Sci* 31(6):643–659
- Nicksiar M, Martin CD (2012) Evaluation of methods for determining crack initiation in compressive tests on low-porosity rocks. *Rock Mech Rock Eng*. doi:10.1007/s00603-012-0221-6
- Palchik V (2007) Use of stress–strain model based on Haldane's distribution function for prediction of elastic modulus. *Int J Rock Mech Min Sci* 44(4):514–524
- Palchik V (2010a) Mechanical behavior of carbonate rocks at crack damage stress equal to uniaxial compressive strength. *Rock Mech Rock Eng* 43(4):497–503
- Palchik V (2010b) Compressive stress levels at which permeability of rock mass increases. In: 6th Conference of institute of mathematics and its applications. Modelling Permeable Rocks. University of Edinburgh, UK, 29 March–1 April, pp 75–78
- Palchik V (2011) On the ratios between elastic modulus and uniaxial compressive strength of heterogeneous carbonate rocks. *Rock Mech Rock Eng* 44(1):121–128
- Palchik V, Hatzor YH (2002) Crack damage stress as a composite function of porosity and elastic matrix stiffness in dolomites and limestones. *Eng Geol* 63(3–4):233–245
- Palchik V, Hatzor YH (2004) The influence of porosity on tensile and compressive strength of porous chalks. *Rock Mech Rock Eng* 37(4):331–341
- Paterson MS (1978) *Experimental rock deformation—the brittle field*. Springer, New York, p 254
- Pettitt WS, Young RP, Marsden JR (1998) Investigating the mechanics of microcrack damage induced under true-triaxial unloading. In: Eurock 98, Society of Petroleum Engineering, pp SPE 47319
- Schock RN, Heard HC, Stevens DR (1973) Stress–strain behavior of a granodiorite and two graywackes on compression to 20 kilobars. *J Geophys Res* 78:5922–5941
- Stefanov YP, Chertov MA, Aidagulov GR, Myasnikov AV (2011) Dynamics of inelastic deformation of porous rocks and formation of localized compaction zones studied by numerical modeling. *J Mech Phys Solids* 59(11):2333–2340